Christoph Neugebauer[1]
Andreas Bück[2]
Achim Kienle[1,3,*]

Control of Particle Size and Porosity in Continuous Fluidized-Bed Layering Granulation Processes

Particle formulation processes such as continuous fluidized-bed layering granulation (FBLG) are widely applied in chemical, food, and pharmaceutical industries. Particle size and particle porosity are important product properties in FBLG. In this paper, a new concept is presented for the simultaneous control of both properties. The new concept allows stable process operation, automatic adjustment of the desired product properties, and rejection of unforseen disturbances.

Keywords: Continuous operation, Fluidized-bed layering granulation, Particle porosity, Particle size, Process stability

Received: August 08, 2019; *accepted:* February 06, 2020

DOI: 10.1002/ceat.201900435

1 Introduction

Fluidized-bed layering granulation (FBLG) is an important class of particle formulation processes. It is widely applied in chemical, food, and pharmaceutical industries. A suspension or solid solution is sprayed into a bed of fluidized particles. The injected liquid evaporates while the solid remains on the surface inducing a layer-wise particle growth.

On the large scale, FBLGs are operated continuously. This allows the formulation of particles with uniform characteristics under steady-state conditions. Continuous product removal requires in turn a continuous supply of new seeds to the granulation chamber. As illustrated in Fig. 1, this can be achieved in combination with an external product classification where the oversized particles are ground in a mill and returned to the process chamber together with the undersized, fine particles as new nuclei. The advantage of the sieve mill cycle is that no external nuclei have to be provided. The disadvantage of the sieve mill cycle is that it can introduce instability in the form of self-sustained oscillations of the particle size distribution, leading to varying product properties which is clearly unwanted in industrial applications [1–4].

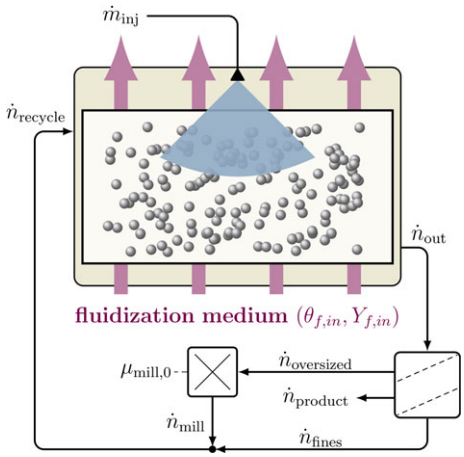

Figure 1. Simplified flowsheet of the continuous fluidized-bed layering granulation process with sieve mill cycle.

In a recent paper, we have shown theoretically and for the first time also experimentally that the particle size distribution can be stabilized elegantly by means of automatic feedback control. This leads also to a considerable improvement of the process dynamics during startup [5]. For this purpose, a linear cascade controller was developed, showing very good performance for small disturbances in the linear range. The results are summarized in Fig. 2. The figure gives a comparison between open loop dynamics without controller and closed loop dynamics with controller. It is demonstrated that the controller dampens the oscillations of the particle size distribution rapidly leading to a stable steady state within short time. More advanced theoretical model based control concepts for larger disturbances were introduced in [6–8].

Besides particle size, particle porosity is an important product specification for FBLG processes. Litster and Ennis [9] pointed out that most of the other particle properties, like

[1]Christoph Neugebauer, Prof. Dr.-Ing. Achim Kienle
kienle@mpi-magdeburg.mpg.de
Otto von Guericke University, Chair for Automation/Modelling, Universitaetsplatz 2, 39106 Magdeburg, Germany.
[2]Prof. Dr.-Ing. Andreas Bück
Friedrich-Alexander University Erlangen-Nuremberg, Institute of Particle Technology, Cauerstrasse 4, 91054 Erlangen, Germany.
[3]Prof. Dr.-Ing. Achim Kienle
Max Planck Institute for Dynamics of Complex Technical Systems, Process Synthesis and Process Dynamics (PSD), Sandtorstrasse 1, 39106 Magdeburg, Germany.

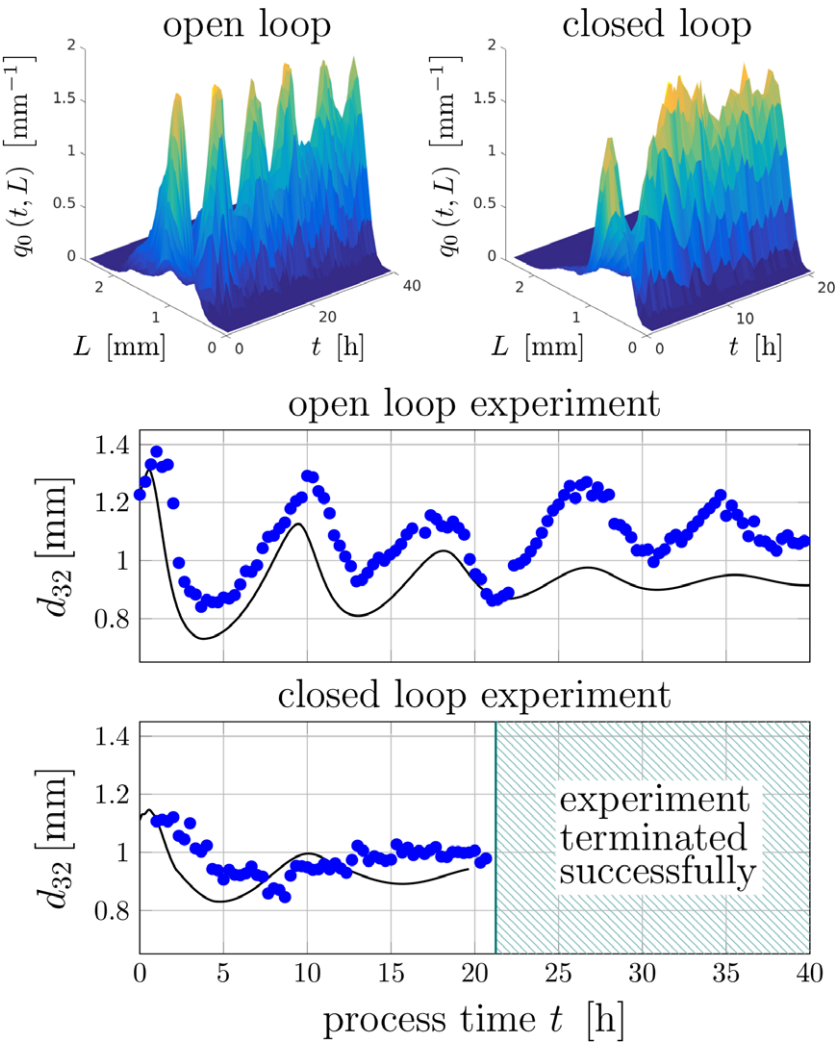

Figure 2. Stabilization of the particle size distribution by feedback control according to [5]. Comparison of open-loop dynamics without control and closed-loop dynamics with feedback control of the Sauter diameter d_{32} by adjustment of the mill power.

particle strength, flowability, and dissolution behavior, essentially depend on particle size and porosity. Particle porosity crucially depends on the thermal operating conditions such as the temperature and the moisture content of the fluidization gas or the injection rate of the solid solution or suspension in FBLG [10]. A quantitative dynamic model to predict the influence of the thermal conditions on the particle properties including the particle size distribution and the porosity was proposed recently in Neugebauer et al. [11]. As described in the experimental work of Schmidt et al. [12], thermal conditions may also influence the process stability, which is not yet taken into account in the model presented in Neugebauer et al. [11]. There, it was conjectured that particle porosity affects the comminution process in the mill, which is known to be crucial for stability. However, a more detailed investigation is lacking up to date.

These gaps will be closed in the present paper. For that purpose, the model of Neugebauer et al. [11] will be extended to account for the influence of the thermal conditions on particle properties and the milling and its effect on process stability. Afterwards, an extended control concept is developed stepwise to adjust the desired particle properties and achieve a stable process operation.

2 Mathematical Model

The following is based on the dynamic model of Neugebauer et al. [11]. The model consists of a population balance equation for the particle size distribution $n(t,L)$ and a set of ordinary differential equations for the thermal conditions in the fluidized bed. The population balance equation accounts for particle growth due to layering granulation and for the in- and outgoing particle fluxes as illustrated in Fig. 1. Following the ideas in [5], the assumption of a constant bed mass was relaxed and a standard PI controller was added to actively control the bed mass by manipulating the rate of the particles withdrawn from the granulation chamber.

The ordinary differential equations represent the energy balances of the fluid and the particle phase, the material balances of the solvent in the fluid, and the particle phase and the dry mass of particles and fluidization gas. The particle and the gas phases are assumed to be well mixed. It is further assumed that all particles, although different in size, share the same average shell porosity $\varepsilon_{\text{shell}}$ and apparent porosity ε_{p}.

Both subsystems are coupled by: (i) the average shell porosity, which depends on the thermal conditions and influences the particle growth and (ii) the total surface of the particle phase $A_{\text{P}} = \pi \int_0^\infty L^2 n(t,L)\mathrm{d}L$ which influences the heat and mass transfer between the phases. For the details the reader is referred to [11].

The model is complemented by models for the classifying screens and the mill. The screens are modeled with static sigmoidal separation functions (see Eqs. (7)–(10) in [11]). The mill is assumed to be mass-conserving with a normal size distribution of the milled particles with mean μ_{mill} and variance σ^2_{mill}. As reported in [13], the particle comminution also depends on the particle porosity, which was not considered so far, but may affect process stability and is therefore crucial for the design of an appropriate control strategy, since stability is the primary objective of any control concept.

In general, the influence of particle porosity on the grinding in the mill depends on the specific equipment, the specific material, and the specific operating conditions. These dependencies are difficult to predict and need to be fitted to the

specific system under consideration. To illustrate the main effects, we will focus here on a simple linear relationship between μ_{mill}[1)] and ε_{p} according to:

$$\mu_{\mathrm{mill}} = \mu_{\mathrm{mill},0} + \Delta\mu_{\mathrm{mill}}(\varepsilon_{\mathrm{p}}) \tag{1}$$

with

$$\Delta\mu_{\mathrm{mill}}(\varepsilon_{\mathrm{p}}) = a_{\mathrm{break}} + b_{\mathrm{break}}\varepsilon_{\mathrm{p}} \tag{2}$$

which can be obtained by linearization from a more detailed nonlinear relation.

The effect of this dependency on process stability is illustrated in Fig. 3 as a function of the milling ($\mu_{\mathrm{mill},0}$) and the thermal conditions. In Fig. 3, the thermal conditions are represented by the gas inlet temperature $\theta_{\mathrm{f,in}}$ and the inlet gas moisture content Y_{in}. The shaded regions in this figure represent unstable steady states with self-sustained oscillations. It is shown that fine milling, i.e., a low value of $\mu_{\mathrm{mill},0}$, leads to instability, whereas coarse milling leads to stable steady states, which is consistent with the results in [1, 2]. Further, it is evident that a high inlet gas temperature leads also to stable steady states whereas a low inlet gas temperature leads to unstable steady states, which is consistent with the experimental observations in [12].

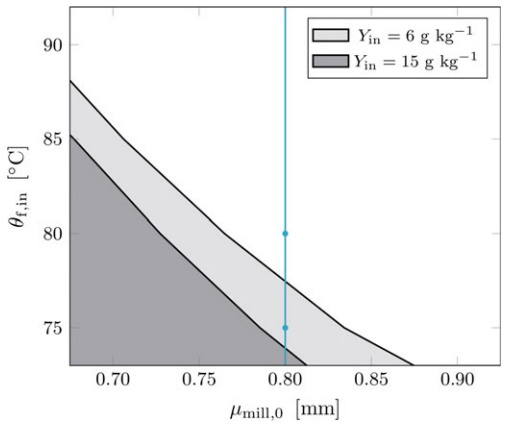

Figure 3. Stability map in the ($\theta_{\mathrm{f,in}}$, $\mu_{\mathrm{mill},0}$) parameter plane. Shaded regions represent unstable steady states. Blue dots symbolize the open-loop simulation experiments in Fig. 7.

The transient from a stable steady state to an unstable steady state is illustrated in Fig. 7 with the black solid line for a change of the gas inlet temperature from 80 °C to 75 °C along the blue line in Fig. 3. The other parameters used in this study are given in Tab. 1.

The response in Fig. 7 clearly demonstrates the influence of the thermal conditions on process stability. Further, the thermal conditions have also great influence on particle properties. This motivates the development of the control concepts to be discussed in the next section.

1) List of symbols at the end of the paper.

Table 1. Plant, model, and controller parameters used in this study.

Parameter	Value
Particle phase	
$c_{\mathrm{p,p}}$ [J kg^{-1}K^{-1}]	4200
Fluidization medium	
$m_{\mathrm{f,dry}}$ [kg]	1
$\dot{m}_{\mathrm{f,dry,in}}$ [kg h^{-1}]	1500
$Y_{\mathrm{f,in}}$ [g$_{\mathrm{wet}}$kg$_{\mathrm{dry\ air}}^{-1}$]	6
$\theta_{\mathrm{f,in}}$ [°C]	95
Injected solution	
$\dot{m}_{\mathrm{inj}}$ [kg h^{-1}]	40
$x_{\mathrm{inj,s}}$ [–]	0.35
θ_{inj} [°C]	20
$\rho_{\mathrm{inj,s}}$ [kg m^{-3}]	1440
Drying characteristics	
τ_{heater} [s]	10
p [–]	0.1
X_{eq} [g$_{\mathrm{wet}}$kg$_{\mathrm{dry\ solid}}^{-1}$]	5
X_{crit} [g$_{\mathrm{wet}}$kg$_{\mathrm{dry\ air}}^{-1}$]	50
$\varepsilon_{\mathrm{shell}}$ [–]	0.45
$\Delta\varepsilon_{\mathrm{shell}}$ [–]	–0.33
Screen, mill, and recycle	
$\mu_{\mathrm{screen,I}}$ [mm]	1.00
$\sigma_{\mathrm{screen,I}}$ [mm]	0.065
$\mu_{\mathrm{screen,II}}$ [mm]	1.40
$\sigma_{\mathrm{screen,II}}$ [mm]	0.055
$\mu_{\mathrm{mill},0}$ [mm]	0.80
σ_{mill} [mm]	0.10
a_{break} [mm]	–2.50
b_{break} [mm]	0.9829
Controller parameters	
$m_{\mathrm{bed,ref}}$ [kg]	15.00
k_{bed} [kg^{-1}]	–0.001
$\tau_{\mathrm{bed,i}}$ [s]	1000
η_{ref} [–]	0.1722
k_{η} [–]	10.0
$\tau_{\eta,\mathrm{i}}$ [s]	100
$d_{32,\mathrm{ref}}$ [mm]	1.12
k_{d32} [–]	0.01
$\tau_{\mathrm{d32,i}}$ [s]	100

3 Control Concepts

The control concepts developed in this section are summarized in Fig. 4. As pointed out above, a basic control loop is required for keeping the bed mass constant. This is achieved with a standard PI controller which manipulates the particle withdrawal from the granulation chamber. In practice, bed mass is measured indirectly by the pressure difference across the bed. For the practical implementation of the bed mass control the reader is referred to [5].

Other control objectives are defined particle sizes and particle porosities. In principle, this is a multivariable control problem with multiple inputs and outputs. However, it will be demonstrated that a decentralized approach gives good performance, i.e., the remaining control loops are designed independently one after another. Due to the different time scales of the sub-processes – thermal dynamics are much faster than the particle dynamics – cross coupling between the control loops is relatively mild and is not explicitly considered for controller design.

First, the focus is on the control of the porosities. The main problem here is that shell and apparent particle porosity cannot be measured online. Therefore, an inferential approach is selected. As indicated in [10], shell porosity is directly related to the drying potential η, which depends on the measurable thermal conditions inside the granulation chamber and can be directly manipulated by the inlet temperature of the gas $\theta_{f,in}$. Therefore, the drying potential is used as a controlled variable and the gas inlet temperature as the manipulated variable. Since the temperature cannot be adjusted instantaneously, the dynamics of the heaters have been modeled as a first-order lag system with a time constant of $\tau_{heater} = 10$ s.

For the controller design, the nonlinear model equations were discretized and linearized around a reference state with $\mu_{mill,0} = 0.8$ mm and $\theta_{f,in} = 80$ °C. This leads to a linear model of order 208. This model was further reduced to an order of 11 using a balanced truncation [14]. The corresponding frequency responses of all four transfer functions are illustrated in Fig. 5 showing good agreement between the full-order and the reduced-order linear model. All calculations were performed in the Matlab environment (2018a, MathWorks, Natick, MA 2018).

Controller tuning was done with the root locus method as indicated in Fig. 6. Controller parameters are given in Tab. 1.

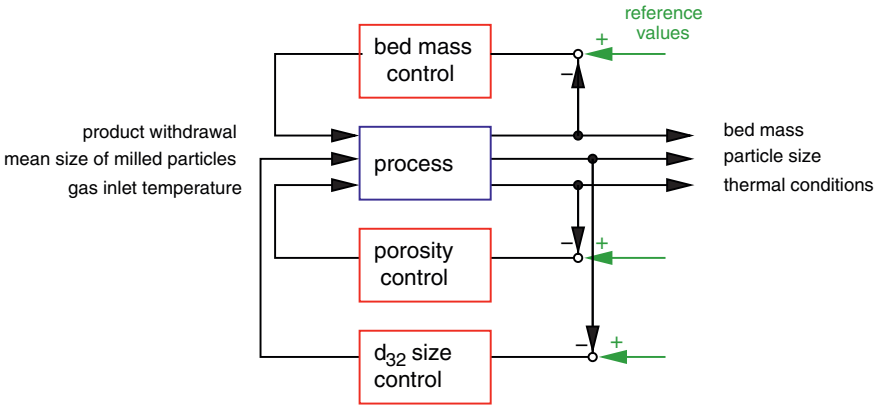

Figure 4. Block diagram of the control strategies used in this paper.

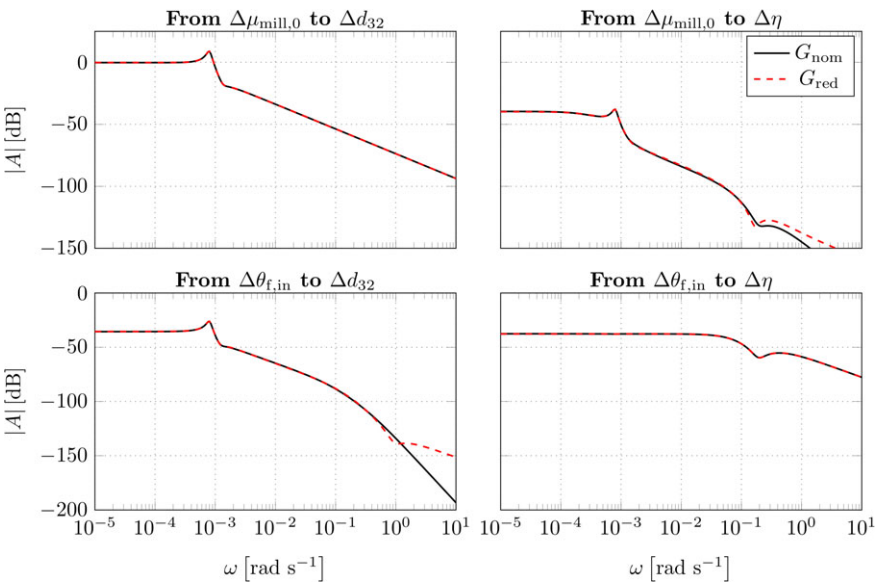

Figure 5. Bode plot of the nominal G_{nom} and the reduced system G_{red}. G_{nom} was obtained by linearization around the reference steady state with $\mu_{mill,0} = 0.8$ mm and $\theta_{f,in} = 80$ °C. Afterwards, G_{nom} of order 208 was reduced to G_{red} of order 11 by balanced truncation.

Root loci for the porosity control loop are displayed in the left diagram of Fig. 6. The open-loop dynamics is stable at the reference point but has some poles close to the imaginary axis, which may lead to instability after changing the reference values or after the occurrence of some permanent disturbances.

The dynamic behavior of the porosity plus the bed mass controller with the full blown nonlinear plant model is illustrated in Fig. 7 with the blue dashed lines. After 2 h the set point of the porosity controller is changed form $\varepsilon_{p,I}$ to $\varepsilon_{p,II}$. The new value is achieved by automatic readjustment of the gas temperature $\theta_{f,in}$ within a relatively short time of about 3 h. Further, a step disturbance of the moisture content of the gas inlet from 6 to 15 g kg^{-1} dry air occurring at time t_{dist} in Fig. 7 is rejected. However, a change of ε_p also results in a change of the breakage behavior of the particles. This leads to instability of the particle size distribution, which is illustrated in the second diagram of Fig. 7 by means of the Sauter diameter d_{32}.

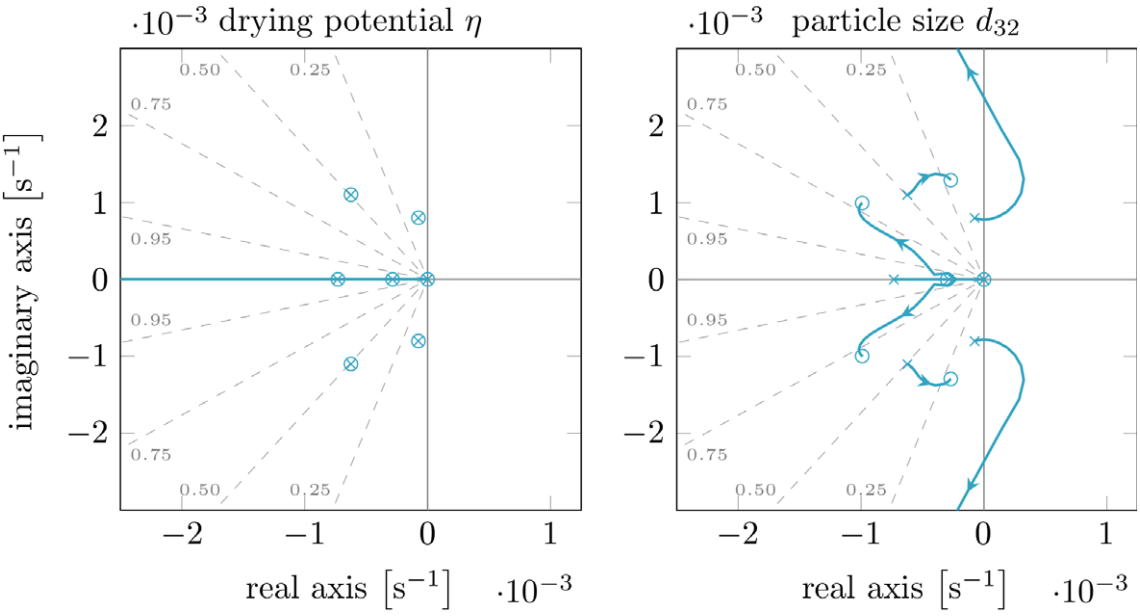

Figure 6. Root loci of the reduced transfer functions (a) $G_{\theta_{f,in} \to \eta}$ and (b) $G_{\mu_{mill,0} \to d_{32}}$.

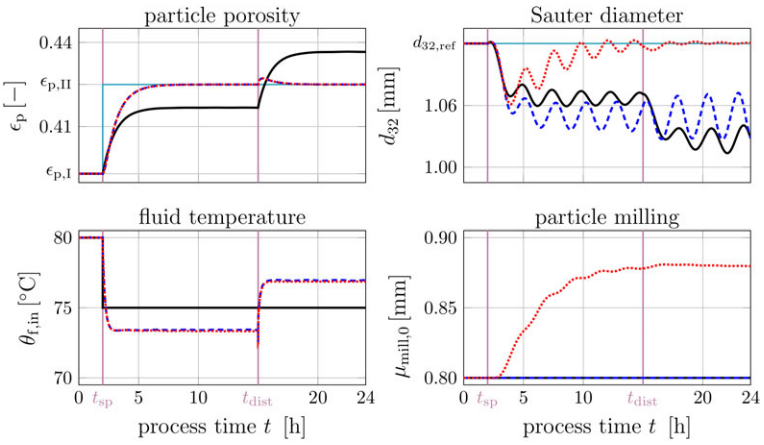

Figure 7. Simulation results: open-loop control (black solid line), closed-loop control of ε_p only (blue dashed line), closed-loop control of ε_p and d_{32} (red dotted line).

To stabilize the particle size distribution, the control strategy is extended by a third controller, which stabilizes d_{32} by manipulation of $\mu_{mill,0}$. The corresponding root loci for this control loop are indicated in Fig. 6 on the right. Again, the reference state is stable, as all open-loop poles are in the left half plane. When the controller gain is increased, a pair of conjugate complex poles moves to the right half plane corresponding to instability. If the gain is further increased, these dominating poles will return to the left half plane and the system is stable again. In consequence, there is a stable range for low controller gains and a stable range for high controller gains. The low controller gain region was selected due to the better damping. Controller parameters are given in Tab. 1.

With the bed mass, the porosity, and the particle size control, finally stable operation with desired particle properties is achieved as illustrated in Fig. 7 with the red dotted line.

4 Conclusion

A new concept for the control of fluidized-bed layering granulation with external sieve mill cycle was presented. The objective was to stabilize the process and to adjust the desired particle size and porosity in the presence of unforeseen disturbances. For this purpose, the mean particle size and thermal conditions were measured online. In contrast, particle porosity was not determined online but directly related to the thermal conditions inside the bed. Therefore, the mean particle size was controlled directly, whereas the particle porosity was controlled indirectly via thermal conditions. The latter is also known under the term inferential control [15]. In addition, the constant bed mass was achieved by regulating the product withdrawal.

The controllers were based on decentralized PI control and showed good performance in view of set point tracking and disturbance rejection in the vicinity of a given reference point. It was further shown that in this range the control concept is robust against plant model mismatch introduced by discrete approximation of the underlying partial differential equation, subsequent linearization, and model order reduction. Future work will focus on nonlinear and robust control to account for larger model uncertainties and disturbances, which may be present during startup operation.

The controller design was based on an extended mathematical model. The influence of particle porosity on breakage

behavior in the mill was explicitly taken into account. With this approach, the influence of thermal conditions on process stability as observed experimentally in [12] could be explained qualitatively. A quantitative description was beyond the scope of this paper and will also be the subject of future work.

Acknowledgment

The financial support of the DFG (Deutsche Forschungsgemeinschaft) within the priority program SPP1679 (project No. Kl 417/3-3) and by the European Regional Development Fund (ERDF) within the Center of Dynamic Systems is gratefully acknowledged.

The authors have declared no conflict of interest.

Symbols used

a,b	[mm]	empirical constants in Eq. (2)
c_p	[J kg^{-1}K^{-1}]	heat capacity
d_{32}	[mm]	Sauter diameter
k	[–]	controller gain
m	[kg]	mass
$\dot{m}$	[kg h^{-1}]	mass flow
p	[–]	material-specific drying parameter as described in [11]
x	[–]	mass fraction of solid
X	[$g_{wet}kg_{dry\ solid}^{-1}$]	moisture content of solid
Y	[$g_{wet}kg_{dry\ air}^{-1}$]	moisture content of gas

Greek letters

ε_p	[–]	average apparent particle porosity
ε_{shell}	[–]	average shell porosity
η	[–]	drying potential
θ	[°C]	temperature
μ	[mm]	mean size
ρ	[kg m^{-3}]	density
σ	[–]	variance
τ	[s]	time constants
τ_i	[s]	integration time constant

Subscripts

bed	particle bed in the granulator
dry	dry content of particles or gas in granulator
g	gas phase
inj	injected solution
mill	mill
p	particle phase
ref	reference value of controller
screen	screen

Abbreviation

FBLG	fluidized-bed layering granulation

References

[1] S. Heinrich, M. Peglow, M. Ihlow, M. Henneberg, L. Mörl, *Chem. Eng. Sci.* **2002**, *57 (20)*, 4369–4390. DOI: https://doi.org/10.1016/S0009-2509(02)00352-4

[2] R. Radichkov, T. Müller, A. Kienle, S. Heinrich, M. Peglow, L. Mörl, *Chem. Eng. Proc.* **2006**, *45 (10)*, 826–837. DOI: https://doi.org/10.1016/j.cep.2006.02.003

[3] C. Dreyschultze, C. Neugebauer, S. Palis, A. Bück, E. Tsotsas, S. Heinrich, A. Kienle, *Particuology* **2015**, *23*, 1–7. DOI: https://doi.org/10.1016/j.partic.2015.02.004

[4] M. Schmidt, C. Rieck, A. Bück, E. Tsotsas, *Chem. Eng. Sci.* **2015**, *137*, 466–475. DOI: https://doi.org/10.1016/j.ces.2015.06.060

[5] C. Neugebauer, E. Diez, A. Bück, S. Palis, S. Heinrich, A. Kienle, *Powder Technol.* **2019**, *354*, 765–778. DOI: https://doi.org/10.1016/j.powtec.2019.05.030

[6] S. Palis, A. Kienle, *Chem. Eng. Sci.* **2012**, *70*, 200–209. DOI: https://doi.org/10.1016/j.ces.2011.08.026

[7] S. Palis, A. Kienle, *J. Process Control* **2014**, *24 (3)*, 33–46. DOI: https://doi.org/10.1016/j.jprocont.2013.12.003

[8] A. Bück, S. Palis, E. Tsotsas, *Powder Technol.* **2015**, *270*, 575–583. DOI: https://doi.org/10.1016/j.powtec.2014. 07.023

[9] *The Science and Engineering of Granulation Processes* (Eds: J. Litster, B. Ennis), Springer, Dordrecht, The Netherlands **2004**.

[10] C. Rieck, T. Hoffmann, A. Bück, M. Peglow, E. Tsotsas, *Powder Technol.* **2015**, *272*, 120–131. DOI: https://doi.org/10.1016/j.powtec.2014.11.019

[11] C. Neugebauer, A. Bück, S. Palis, L. Mielke, E. Tsotsas, A. Kienle, *Processes* **2018**, *6 (12)*, 235. DOI: https://doi.org/10.3390/pr6120235

[12] M. Schmidt, A. Bück, E. Tsotsas, *Powder Technol.* **2017**, *320*, 474–482. DOI: https://doi.org/10.1016/j.powtec.2017.07.012

[13] E. Diez, K. Meyer, A. Bück, E. Tsotsas, S. Heinrich, *Chem. Eng. Res. Des.* **2018**, *139*, 104–115. DOI: https://doi.org/10.1016/j.cherd.2018.09.032

[14] *Multivariable Feedback Control* (Eds: S. Skogestad, I. Postlethwaite), 2nd ed., John Wiley & Sons, Chichester **2005**.

[15] G. Stephanopoulos, *Chemical Process Control*, Prentice Hall, Upper Saddle River, NJ **2001**.

